MASTER OF PHILOSOPHY, Modelling of Materials

Thursday 26 April 2001 9 – 12

MODELLING OF MATERIALS (1) – possible Answers

SECTION A

1. (a) Integer variables hold integer values precisely (over a finite range).

Real variables hold a much wider range of values (which need not be integer) approximately. A quantity called the machine epsilon is the smallest number which, when added to 1.0, differs from 1.0 (using machine arithmetic).

[Certain values, called model numbers, are stored precisely, though this hasn't been mentioned to the students.]

```
integer i
real sum
sum = 0.0

do 10, i = 100, 1, -1
  sum = sum + 1.0 / real (i)
10 continue
write (*,*) 'sum of reciprocals is ', sum
end
```

Note: It is more accurate to sum the values starting with the smallest first, though the students are not expected to be aware of this.

(b) Given a maximum plane strain plastic zone size of $0.16(K/\sigma)^2$, the maximum extent of the plastic zone cannot exceed about 1/15 of the specimen thickness. Plots of toughness versus testpiece thickness have demonstrated that this is sufficient to ensure that measurements are made on the lower shelf of the toughness curve.

The requirement of the in–plane dimensions, principally that

$$a \quad \& \quad (W-a) \geq 2.5(K_{1c}/\sigma_y)^2$$

is to ensure that the nominal behaviour is linear–elastic and K characterises the crack tip conditions. Here a is the crack length and W is the specimen width.

(c) The elastic modulus depends on the bonding between atoms, specifically the way in which the force between the atoms varies as a function of interatomic separation. It does not depend, for example, on

the defect structure of the material. The yield strength on the other hand is sensitive to the microstructure. An *ab initio* method is used to model the elastic modulus whereas the yield strength would involve a consideration of factors such as the dislocation density, grain size, precipitate strengthening, solid solution strengthening *etc.*

(d) Casting involves the solidification of the alloy, often by pouring liquid metal into a mould. The rate of formation of the solid is then controlled by the rate at which heat is extracted from the melt.

Commercial alloys contain many solutes. Examples include (i) steels which consist of Fe alloyed with C, Mn, Si ... and (ii) the superalloys which consist of Ni alloyed with Ti, Al, Ta, W .....

A basic consideration of the form of the phase diagram in these systems shows that (i) the melting temperature is a function of the solute content and (ii) solute partitions between solid and liquid phases as transformation proceeds.

Consider a case where the solid is richer in solute than the liquid, and where the liquidus temperature is depressed by the solute. There is a need for solute diffusion to occur in the liquid ahead of the solid/liquid interface: a composition gradient exists which depends upon the phase diagram, the growth velocity, the mean composition and the diffusion coefficient of solute in the liquid. Consequently, the *local* melting temperature of the liquid ahead of the interface increases with increasing distance from the interface. Under conditions of positive temperature gradient, the interface can then be unstable with respect to perturbations since the local temperature ahead of the interface is lower than the equilibrium melting temperature. This is known as *constitutional supercooling*. Interfaces are prone to this effect at high velocities and low values of the temperature gradient.

(e) An ideal solution is one where the enthalpy of mixing is zero so that the configurational entropy can be calculated assuming a random distribution of atoms. The enthalpy of mixing is non–zero in a regular solution. It follows that the atoms have a preference for particular species of neighbouring atoms so the distribution of atoms cannot be random except at high temperatures where entropy favours mixing. Nevertheless, the configurational entropy is estimated assuming a random distribution of atoms, which may be an unacceptable approximation if the enthalpy of mixing is large.

(f) The principal steps can be summarised as follows:

Identifying the problem (target phenomenon of interest)

Inputs/outputs (the essential ingredients)

Identifying physical mechanisms (assumed mechanisms should be tested)

Target precision (what precision is tolerable?)

Construct model (choose length scale and methodology)

Dimensional analysis (check units)

Computer implementation (efficient coding)

Interrogation of model (model validation)

Display results (visualisation, movies)

(g) Principal terms comprising the total energy $E[n(r)]$ of a solid using DFT:

$$E[n(r)] = T[n(r)] + E_{ext}[n(r)] + E_H[n(r)] + E_{XC}[n(r)]$$

where $n(r)$ is the single particle (electronic) density; $T[n(r)]$ is the kinetic energy of the non–interacting electrons; $E_{ext}[n(r)]$ is the Coulomb interaction between the electrons and the ions; $E_H[n(r)]$ is the Coulomb energy of the electron density (Hartree energy); $E_{XC}[n(r)]$ is the exchange–correlation energy.

Traditional method for minimising the total energy: Construct the single particle wave equations (the Kohn–Sham equations). These have the form

$$H|\psi_I >= \epsilon_I|\psi_I >$$

where H is the Hamiltonian comprising the kinetic energy operator, the electron–ion potential, the Hartree potential and the exchange–correlation potential. The single particle eigenvalues and eigenfunctions are given by ϵ_I and ψ_I. This is an eigenvalue equation which is solved traditionally by diagonalising the Hamiltonian matrix.

Modern method for minimising the total energy: Conventional diagonalisation is too slow and computationally demanding for more than a few dozen atoms. In addition the traditional approach does not allow for calculating forces on ions and therefore the ionic configuration is frozen. To speed up the convergence and to allow for atomic relaxation as well as electronic relaxation modern methods use iterative diagonalisation. The energy gradient is calculated at each iteration and the total energy is minimised by systematically adjusting the gradients using a modified method of steepest descents, known as conjugate gradients. The atomic forces can be calculated using the Hellmann-Feynman theorem and the atomic positions can be adjusted to minimise the energy using either conjugate gradients

again or molecular dynamics (simulated annealing). The modern method allows system sizes of several hundred atoms to be fully optimised.

(h) Normally,

$$\Delta S^0_T = \Delta S^0_{298} + \int \frac{c_P}{T}\, dT$$

Therefore, the entropy change is independent of temperature only when Δc_P, which is the difference between the heat capacities of the products and reactants, is zero.

(i) Statistical temperature T_S is defined in a Monte Carlo simulation by the *equilibrium* microstate distribution, which should be a Boltzmann (or Gibbs) distribution with occupancy probabilities $p_i = Z^{-1}\exp(-E_i/k_BT_S)$, where E_i are the microstate energies, k_B is the Boltzmann constant and Z is the partition function.

Kinetic temperature T_K is defined in a molecular dynamics simulation by the average *equilibrium* kinetic energies of the particles $\frac{1}{2}\sum_{i=1}^{N} m_i\langle v_i^2\rangle = Nk_BT_K$, where N is the total number of particles, m_i is the mass of the ith particle and v_i the corresponding velocity.

Strictly speaking, statistical and kinetic temperatures only constitute a measure of thermodynamic temperature once the simulations have reached thermal equilibrium. Statistical temperature is a static property of the system, and relates to its informational entropy, whereas kinetic temperature is a dynamical property that is related to the thermal motion in the system.

(j) The advantage of modelling materials at the atomistic level is that it is possible to describe the fundamental mechanisms that underlie interesting bulk material properties. For example: diffusive and displacive phase transitions, repetitive motion in polymers and electrolyte diffusion, amongst many others. In addition, one has complete access to the static and dynamical variables of the system in a way that is impossible to achieve in a real experiment. The effects of changing individual parameters can be isolated by carrying out 'unphysical simulations, which would be very difficult to do otherwise. It is therefore often easier to compare theory with modelling experiments and, where the results disagree, to understand the deficiencies of either approach.

The disadvantage of atomistic modelling is that it is quite computationally expensive and therefore difficult to study situations that involve much more than a million atoms. For example, crack propagation in solids is a problem that has only recently been amenable to direct simulation due to the vast degree of cooperative motion at the atomistic scale. This, and other emergent phenomena, are

better studied by linking together time and length scales with a coarse–grained modelling approach. However, computer technology is advancing all the time, and the number of problems that can be tackled at the atomistic level is increasing on a daily basis.

SECTION B

2. Strength can refer to the yield strength or the ultimate tensile strength. The former is a measure of the ability of the material to sustain a stress without permanent deformation. The ultimate tensile strength represents the maximum engineering stress that a sample can support. Toughness, on the other hand, is a measure of the ability of the material to absorb energy on fracture. Strength is measured using a tensile specimen which is taken to fracture whilst monitoring the load versus extension of the sample. Toughness can be characterised empirically using a Charpy impact test, in which the energy absorbed by a smoothly notched sample subjected to an impact load is measured. Alternatively it can be measured as a material property using a fracture toughness specimen which is sufficiently large to ensure a valid result. The sample in this case contains a sharp crack.

   The expression for the stress distribution ahead of a sharp crack has to be modified for bodies of finite size to allow for plastic relaxation at free surfaces.

   The critical value of the stress intensity at which fracture occurs is

$$K_{1c} = 1.12 \times 100 \times (\pi \times 0.04)^{\frac{1}{2}} = 39.7\,\mathrm{MPa\,m}^{\frac{1}{2}}$$

   The circular hole would introduce a stress concentration, thereby reducing the magnitude of the applied stress at which fracture occurs. There is a dependency on the size of the crack relative to that of the hole.

3. Bonding in ionic crystals results from electrostatic interactions between oppositely charged ions $\pm q2/r$ (long range, pairwise, attraction and repulsion). Alkali halides are typical.

   Valence electron distributions are spherical, highly localised and similar to free atoms. However electron transfer occurs to form complete electron shells. This leaves material composed of $+ve$ and $-ve$ ions. In the case of KCl, one of the valence electrons on the K atom transfers to the Cl atom giving both atoms 18 electrons but leaving K $+ve$ly charged and Cl $-ve$ly charged.

   KCl is a typical insulator with a large band gap. Its band structure is characterised by a completely full valence band and a completely empty conduction band.

   The spherical nature of the valence electron distribution means that, to a good approximation, the interatomic potentials will be spherically symmetric (*i.e.* radial and pairwise) and will be dominated by the $1/r$ Coulombic interaction. Refinements to this potential are the inclusion of a short range repulsive term (Born-Mayer potential), a weak attrac-

tive term (van der Waals), and a harmonic term to account for atomic polarisation (shell potential).

At equilibrium $(du/dr)_{r=r_0} = 0$ so that

$$\frac{\alpha q^2}{r_0^2} + mCr_0^{m-1} = 0 \qquad \text{therefore} \qquad C = -\frac{\alpha q^2}{mr_0^{m+1}}.$$

At equilibrium

$$u(r_0) = -\frac{\alpha q^2}{r_0} - \frac{\alpha q^2 r_0^m}{mr_0^{m+1}} = -\frac{\alpha q^2}{r_0}\left(\frac{m+1}{m}\right)$$

If 90% of the cohesive energy of KCl is Coulombic, then 10% is due to the core–core repulsion. The Coulombic energy makes a negative contribution to the total cohesive energy (which itself is negative) and the core–core repulsive term makes a positive contribution. For example, for KCl:

$$\underbrace{u(r_0)}_{-1.15} = \underbrace{u(\text{Coulombic})}_{-1.28} + \underbrace{u(\text{core–core})}_{0.13\ \text{eV}}$$

Thus, the ratio of the core–core term to the Coulombic term is $-1/9$ so that

$$\frac{-\alpha q^2}{mr_0} \Big/ \frac{-\alpha q^2}{r_0} = -\frac{1}{9} \qquad \text{and} \qquad m = -9$$

4. The free energy of formation of metallic oxides is less negative at high temperatures because for the typical reaction

$$\mathrm{M} + \mathrm{O_2} \rightarrow \mathrm{MO_2} \qquad \text{with} \qquad \Delta G = \Delta H - T\Delta S,$$

ΔS is large and negative since one mole of gas ends up in solid oxide. Since $-T\Delta S$ is large and positive, when added to the negative ΔH results is a less negative ΔG. However, rates of oxidation are controlled by kinetic phenomena such as diffusion, processes which are thermally activated. These become easier at elevated temperatures and therefore oxidation occurs more rapidly.

The standard free energy change ΔG^0 is given by

$$\Delta G^0(1000\,\mathrm{K}) = -195000\,\mathrm{J\,mol^{-1}}\ \text{of oxygen} = -RT\ln K$$

where K is the equilibrium constant. Therefore, $K = 1.53 \times 10^{10}$ and thus $p_{O_2} = K^{-1} = 6.54 \times 10^{-11}$ atm.

If iron is made impure, *i.e.,* the activity of iron is less than 1, the equilibrium partial pressure of oxygen will increase to maintain the equilibrium constant at the same value at a given temperature.

5. A force field is a potential energy function for a molecular system that includes all of the internal degrees of freedom of each molecule, together with terms describing the interactions between molecules. In order to be useful, a force field must be simple enough that it can be evaluated quickly, but sufficiently detailed that it is capable of reproducing the salient features of the system being modelled. Although force fields are entirely classical in nature, they can mimic the behaviour of atomistic systems with an accuracy which approaches that of the highest level of quantum mechanical calculations if parameterised accurately.

   A suitable force field expression for a long–chain polymer molecule might be:

$$\begin{aligned} V =& \frac{k_b}{2}(r_{ij} - r_0)^2 + \frac{k_\theta}{2}(\theta_{ijk} - \theta_0)^2 + \frac{k_\phi}{2}(1 + \cos 3\phi_{ijk}) \\ &+ D_0\left\{\left(\frac{R_0}{r_{ij}}\right)^{12} - 2\left(\frac{R_0}{r_{ij}}\right)^{6}\right\} + \frac{q_i q_j}{4\pi\epsilon_0 r_{ij}} \end{aligned}$$

   where the k are force constants, r_{ij} the interatomic separations, θ_{ijk} the angles between adjacent triplets of bonded atoms, ϕ_{ijk} the dihedral angles between adjacent quartets of bonded atoms, D_0 the well–depth and R_0 the equilibrium separation for the van der Waals interactions and q the electrostatic charges on the atoms. The first three terms are called bonded terms, and represent the internal degrees of freedom of the molecule, and the last two terms are the non-bonded terms, and represent the interactions between molecules. Note that more complex functional forms for the various terms, such as the triply harmonic torsional potential, are also acceptable in lieu of the more simple forms quoted here. There may also be differences in the notation used for the van der Waals interaction.

   The RIS model, due to Flory, is a model for polymer conformations based on a Boltzmann distribution of torsional states in the molecule. Assuming that adjacent states are independent, the probability distribution of the dihedral angles ϕ along the chain is given by:

$$p(\phi) = \frac{1}{Z_{RIS}} \exp\left\{-\frac{V(\phi)}{k_B T_{RIS}}\right\}$$

   where Z_{RIS} is the RIS partition function, $V(\phi)$ is the torsional potential and T_{RIS} is the RIS temperature. The RIS temperature is a form of statistical temperature, which relates to the degree of configurational disorder possessed by the chain.

SECTION C

6. When most of the driving force is dissipated in diffusion, the interface is said to move at a rate *controlled* by diffusion. Interface–controlled growth occurs when most of the available free energy is dissipated in the process of transferring atoms across the interface.

These concepts are illustrated in Fig. 1, for a solute–rich precipitate β growing from a matrix α in an alloy of average chemical composition C_0. The equilibrium compositions of the precipitate and matrix are respectively, $C^{\beta\alpha}$ and $C^{\alpha\beta}$.

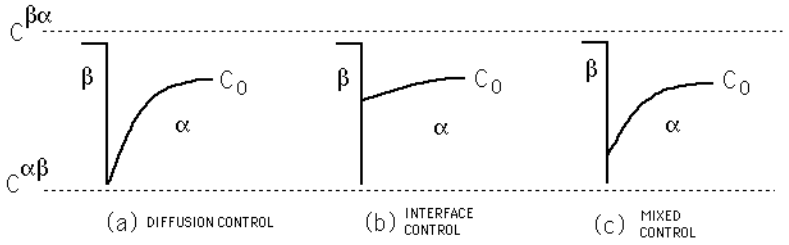

Fig. 1:Concentration profile at an α/β interface moving under: (a) diffusion–control, (b) interface–control, (c) mixed interface.

A reasonable approximation for diffusion–controlled growth is that local equilibrium exists at the interface. On the other hand, the concentration gradient in the matrix is much smaller with interface–controlled growth because most of the available free energy is dissipated in the transfer of atoms across the interface.

The diffusion flux of solute towards the interface must equal the rate at which solute is incorporated in the precipitate so that:

$$\underbrace{(C^{\beta\alpha} - C^{\alpha\beta})\frac{\partial x^*}{\partial t}}_{\text{rate solute absorbed}} = \underbrace{D\frac{\partial C}{\partial x}\bigg|_{x=x^*}}_{\text{diffusion flux towards interface}} \simeq D\frac{C_0 - C^{\alpha\beta}}{\Delta x}$$

where Δx is the diffusion distance in the matrix ahead of the interface assuming a constant gradient. A second equation can be derived by considering the overall conservation of mass:

$$(C^{\beta\alpha} - C_0)x^* = \frac{1}{2}(C_0 - C^{\alpha\beta})\Delta x$$

On combining these expressions to eliminate Δx we get:

$$\frac{\partial x^*}{\partial t} = \frac{D(C_0 - C^{\alpha\beta})^2}{2x(C^{\beta\alpha} - C^{\alpha\beta})(C^{\beta\alpha} - C_0)}$$

If, as is often the case, $C^{\beta\alpha} \gg C^{\alpha\beta}$ and $C^{\beta\alpha} \gg C_0$ then

$$2\int x^* \partial x^* = \left(\frac{C_0 - C^{\alpha\beta}}{C^{\beta\alpha} - C^{\alpha\beta}}\right)^2 D \int \partial t \quad \text{so that} \quad x^* \simeq \frac{\Delta C_{ss}}{\Delta C_{\alpha\beta}}\sqrt{Dt}$$

As the solute concentration in the precipitate approaches the average concentration, the equations predict an infinite growth rate. This is not realistic because other rate–controlling processes become limiting.

The equation would fail if the boundary conditions changed, for example, if the matrix ahead of the particle was finite in extent so that soft–impingement occurred.

7. The Jominy end–quench is used to measure the hardenability of a steel, *i.e.* its ability to form martensite during continuous cooling from the austenite field on the phase diagram. The end–quench generates a wide range of cooling rates in one specimen, with cooling rate falling with distance from the quenched end. Hardenability depends on the position of the C–curves on a temperature–time CCT diagram. Low hardenability means high cooling rates are required to avoid these transformations; high hardenability means martensite forms even when the cooling rate is low (*i.e.* at greater distances along the Jominy bar, corresponding to larger cross–sections of a steel component which can be hardened through–thickness).

   Required material properties: thermal conductivity λ and specific heat capacity ρc (either representative constant value, or as function of temperature). Boundary conditions: perfect heat transfer imposed by assigning constant temperature to node 1 of 20 °C; perfect insulation on the sides is imposed automatically by using 1–D elements (since there is then only axial heat flow allowed).

   Plot of results below – note that temperature is linear between the nodes, not a smooth curve. Limitations of this model: – only 2 elements gives crude piecewise linear temperature profile – constant thermal properties assumed, rather than temperature-dependent – ignores heat loss from sides and far end of bar

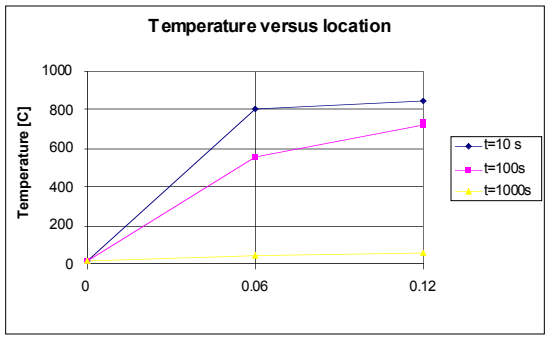

   Refinements: use more elements in the length direction, and grade the mesh to be finer near the quenched end where cooling rates are high; use axisymmetric mesh with a few elements across the radius, to allow for some radial heat flow and convective/radiative heat transfer on the sides of the bar; use temperature–dependent thermal properties; use good but not perfect heat transfer boundary condition on quenched end (with a suitable heat transfer coefficient); adjust time stepping to give temperature values which are sufficiently close together in time (at the positions of interest) to enable a smooth temperature–time profile to be plotted and differentiated, around the critical temperatures of interest from the

point of view of CCT behaviour (*e.g.* 800-500 °C).

Number of tests in a day: use initial 1D analysis, perhaps refined to 10 elements would allow a reasonable estimate of cooling time (*e.g.* time for far end to reach 200 °C, after which a full water quench could be applied to end the test). The analytical error function solution might be considered good enough, but tends to over-estimate cooling time considerably (due to semi–infinite rather than finite bar).

Cooling rate 1 mm from end to high accuracy: this would require the most complex model, with all refinements: surface cooling rate 1 mm from end will be very sensitive to end and side heat transfer conditions, temperature-dependent properties, mesh refinement *etc.*

Adaptation of test to aluminium: similar complexity to the first case (10 or more 1D elements), but with refined time–stepping as cooling rate is of interest, not just overall cooling time. Constant thermal properties OK, and 1D analysis less of a concern in aluminium as temperatures are lower so convective/radiative heat transfer from the sides will be weaker than in steel.